JOURNAL OF NATURAL PRODUCTS

Article

Cite This: J. Nat. Prod. 2019, 82, 45−50

pubs.acs.org/jnp

Tricholopardins A and B, Anti-inflammatory Terpenoids from the Fruiting Bodies of *Tricholoma pardinum*

Tao Feng,[†] Xiao-Qing Gan,[†] Yun-Li Zhao,[‡] Shuai-Bing Zhang,[†] He-Ping Chen,[†] Juan He,[†] Yong-Sheng Zheng,[†] Huan Sun,[†] Rong Huang,[†] Zheng-Hui Li,*[,†] and Ji-Kai Liu*[,†]

[†]School of Pharmaceutical Sciences, South-Central University for Nationalities, Wuhan 430074, People's Republic of China

[‡]State Key Laboratory of Phytochemistry and Plant Resources in West China, Kunming Institute of Botany, Kunming 650201, People's Republic of China

Supporting Information

ABSTRACT: Two new *Tricholoma* terpenoids, tricholopardins A and B, were isolated from the fruiting bodies of the basidiomycetes *Tricholoma pardinum*. Their structures were elucidated by spectroscopic methods, as well as electronic circular dichroism and optical rotatory dispersion calculations. Tricholopardin A potently inhibited nitric oxide production in lipopolysaccharide-induced RAW264.7 macrophages with an IC_{50} of 0.08 μM. Its anti-inflammatory effects on three inflammatory mediators were also evaluated. A plausible biosynthetic pathway for these products is discussed.

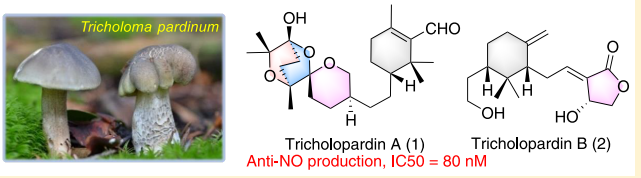

In 1988, De Bernardi et al. reported an interesting triterpenoid, saponaceolide A, from the mushroom *Tricholoma saponaceum*.[1] This compound possessed a novel carbon skeleton in which a central methylenecyclohexane is linked to two heterocycles; the γ-lactone substituent and a pyran shared a spiroketal carbon with the bridged heterocyclic system. A unique biosynthetic pathway was proposed for this compound in which the two farnesyl units were not linked by the tail-to-tail coupling typically seen in the squalene biosynthesis derivatives, the common precursors of triterpenes.[1] Since the publication of that report, six additional analogues, saponaceolides B−G, were reported from the same species.[2−4] A few related synthetic studies have been reported, and a total synthesis of saponaceolide B was achieved.[5−9] In 2014 and 2015, our group identified 18 new compounds from *T. terreum* including terreolides D−F, which have novel carbon skeletons.[10,11] Thus, only 25 related structures have been reported. All these compounds were obtained from mushrooms of the genus *Tricholoma*, and we named them *Tricholoma* terpenoids.

Previous studies also proved that many *Tricholoma* terpenoids exhibited significant cytotoxicities to human cancer cell lines. Saponaceolides A−C inhibited human colon adenocarcinoma,[1−3] while saponaceolide Q was cytotoxic to four human cancer cell lines (HL-60, SMMC-7721, MCF-7, and SW480).[11] In addition, saponaceolides B and M were identified as mushroom toxins that increased serum CK levels in mice.[10]

These properties of *Tricholoma* terpenoids motivated us to investigate other species of the genus *Tricholoma*. Previously, we studied the chemical constituents of the fruiting bodies of *T. matsutake*. There were no *Tricholoma* terpenoids found in this species, but two novel steroids were isolated and reported.[12] Subsequently, a phytochemical study on the fruiting bodies of the mushroom *T. pardinum* led to the isolation of a C25 terpenoid, tricholopardin A (**1**), and a C17 terpenoid, tricholopardin B (**2**), together with a known compound, saponaceolide A. Their structures were elucidated by extensive spectroscopic analyses, as well as electronic circular dichroism (ECD) and optical rotatory dispersion (ORD) calculations. Compound **1** potently inhibited nitric oxide (NO) production in lipopolysaccharide (LPS)-induced RAW264.7 macrophages with an IC_{50} of 0.08 μM. Its inhibitory effects on three inflammatory mediators were also evaluated. Herein we reported the isolation, structural elucidation, and bioactivities of these two new compounds.

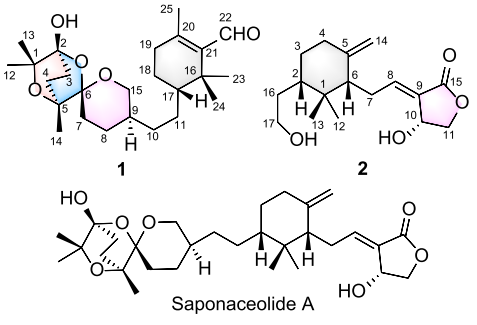

RESULTS AND DISCUSSION

One kilogram of dry *T. pardinum* was extracted with EtOH and partitioned into water and EtOAc. The EtOAc layer was

Received: June 5, 2018
Published: January 10, 2019

DOI: 10.1021/acs.jnatprod.8b00460
J. Nat. Prod. 2019, 82, 45−50

fractionated repeatedly by column chromatography to afford two pure compounds, tricholopardins A (**1**) and B (**2**).

Tricholopardin A (**1**) was isolated as a colorless oil. Its molecular formula ($C_{25}H_{40}O_5$) was determined based on positive mode high-resolution electrospray ionization mass spectrometry (HRESIMS) data, corresponding to six degrees of unsaturation. The IR absorption bands at 3440 and 1717 cm^{-1} revealed the presence of hydroxy and carbonyl functionalities. The majority of the ^1H NMR signals were concentrated in a narrow range (δ_H 0.9−2.3, Table 1). Six

Table 1. ^1H (600 MHz) and ^{13}C (150 MHz) NMR Data for Tricholopardins A (1) and B (2)

	tricholopardin A (**1**)[a]		tricholopardin B (**2**)[b]	
no.	δ_C, type	δ_H (J in Hz)	δ_C, type	δ_H (J in Hz)
1	77.5, C		40.8, C	
2	96.6, C		45.6, CH	1.40, m
3a	27.8, CH_2	2.01, m	32.1, CH_2	1.83, m
3b		1.88, m		1.21, m
4a	28.5, CH_2	2.17, m	38.7, CH_2	2.35, m
4b		1.68, m		2.05, m
5	72.8, C		150.0, C	
6	101.2, C		55.4, CH	2.03, m
7a	29.2, CH_2	1.98, m	27.3, CH_2	2.72, m
7b		1.51, m		2.67, m
8	24.9, CH_2	1.58, m	150.1, CH	6.88, m
9	35.7, CH	1.55, m	130.2, C	
10a	31.2, CH_2	1.32, m	67.1, CH	5.02, d (6.1)
10b		1.05, m		
11a	26.1, CH_2	1.59, m	76.7, CH_2	4.47, dd (10.2, 6.1)
11b		0.90, m		4.17, dd (10.2, 1.9)
12	25.9, CH_3	1.30, s	27.3, CH_3	1.09, s
13	22.4, CH_3	1.21, s	15.6, CH_3	0.66, s
14	20.8, CH_3	1.09, s	109.4, CH_2	4.92, s; 4.68 s
15a	65.9, CH_2	3.71, br d (11.0)	173.2, C	
15b		3.62, br d (11.0)		
16a	36.4, C		35.4, CH_2	1.84, m
16b				1.12, m
17	45.9, CH	1.10, m	62.5, CH_2	3.62, m
				3.52, m
18a	22.5, CH_2	1.70, m		
18b		1.30, m		
19a	35.0, CH_2	2.24, m		
19b		2.18, m		
20	155.7, C			
21	140.9, C			
22	192.7, CH	10.11, s		
23	25.9, CH_3	1.23, s		
24	20.8, CH_3	1.04, s		
25	19.4, CH_3	2.09, s		

[a]Measured in $CDCl_3$. [b]Measured in methanol-d_4.

methyl singlets can be readily identified, and one of them was attached to a double bond based on the characteristic shift at δ_H 2.09. In addition, the signals at δ_H 3.62 and 3.71 could be attributed to protons on the oxygenated carbon, while the signal at δ_H 10.11 revealed the presence of an aldehyde group. With the aid of DEPT and HSQC spectra, 25 carbon resonances as displayed by the ^{13}C NMR spectrum could be ascribed to six CH_3, nine CH_2 (including one oxygenated carbon), three CH (including one aldehyde carbon), and seven C (including two olefinic carbons) (Table 1). Considering one double bond and one aldehyde carbon, compound **1** was supposed to possess a tetracyclic ring system.

In the ^{13}C NMR spectrum of **1**, signals at 96.6 (s) and 101.2 (s) were attributed to the carbons of acetal (or ketal) groups. The $^1H-^1H$ COSY data revealed the two spin systems indicated by bold lines in Figure 2. These data, as well as the

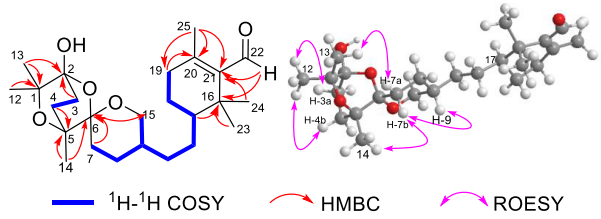

Figure 1. Key 2D NMR correlations of compound **1**.

HMBC correlations from H-12 and H-13 to C-1 and C-2, from H-3 to C-2, from H-4 and H-14 to C-5, from H-14 to C-6, and from H-15 and H-7 to C-6, suggested that **1** should contain a pyran that shared a spiroketal carbon with a bridged 2,5-dioxabicyclo[2.2.2]octane system, which was the same core as seen in saponaceolide A.[1] As shown in Figure 1, the sp^3 carbon at δ_C 36.4 (s) was assigned as C-16 based on the HMBC correlations from H-23 and H-24 to C-16. It was hypothesized to be connected to C-17 based on the HMBC cross-peak from H-17 to C-16. A 20(21)-unsaturated-22-aldehyde moiety was identified by analysis of 1D NMR data and the HMBC correlation from H-22 to C-21. In addition, the HMBC correlations of H-19/C-20, H-22/C-16, H-23/C-21, and H-24/C-21 revealed the fragments of $-CH_2(19)$-C(20)− and −C(16)−C(21)−. These data indicated a substituted cyclohexane containing carbons C-16 to C-21. A methyl connected to C-20 was also suggested by the HMBC correlations from H-25 to C-20, C-21, and C-19. Therefore, the planar structure of **1** was identified.

The stereochemistry of **1** was established from the ROESY experiment in conjunction with the ECD analysis. In the ROESY spectrum (Figure 1), the cross-peaks of H-12/H-3a, H-12/H-4b, H-13/H-7a, and H-14/H-7b suggested that the relative configuration of spiroketal carbon C-6 and the orientation of bridged heterocyclic system were the same as those in the known *Tricholoma* terpenoids.[1−4,10,11] In addition, the key cross-peak of H-7b/H-9 suggested that H-9 and H-7b were axial, which indicated the bond between C-9 and C-10 was equatorial. An energy-minimized 3D structure was consistent with the ROESY cross-peaks (Figure 1). Since the absolute configurations of C-2, C-5, C-6, and C-9 have been determined in saponaceolide A, the similar NMR data and the ROESY analyses of **1** suggested the absolute configuration of C-2, C-5, C-6, and C-9 in **1** to be 2*S*, 5*S*, 6*S*, and 9*S*. However, the configuration of C-17 could not be assigned from the ROESY data. Finally, the absolute configuration of C-17 was determined from its calculated ECD curve using the methods we reported previously, with minor modifications (Figure 2; see the Supporting Information).[12] The ECD spectra of the major conformers were calculated using time-dependent density functional theory (TDDFT) at the CAM-B3LYP/6-311+G(d,p) level in methanol with the PCM model. The calculated ECD spectra of **1a** and **1c** were quite similar, while the spectra of **1a** and **1b** were quite different. These data suggested that the absolute configurations of C-2, C-5, C-6,

DOI: 10.1021/acs.jnatprod.8b00460
J. Nat. Prod. 2019, 82, 45−50

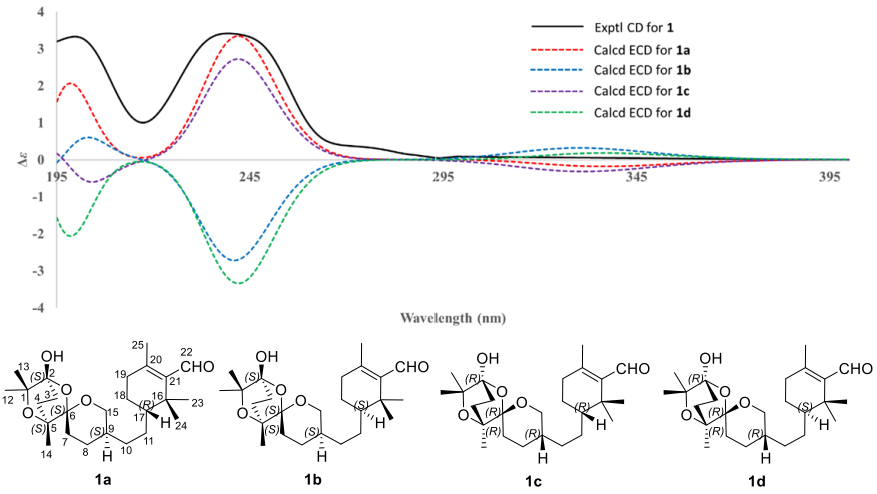

Figure 2. Comparison of the calculated ECD spectra with the PCM model for **1a**, **1b**, **1c**, and **1d** with the experimental spectrum of **1** in methanol.

and C-9 contributed little to the ECD spectrum, while the absolute configuration of C-17 contributed significantly to the ECD spectrum. Therefore, the absolute configuration of C-17 was determined as *R* form from calculated ECD spectra of **1a** and **1c**.[13,14] Moreover, to establish the absolute configurations of **1**, the specific rotations ($[\alpha]_D$) of the two possible structures **1a** and **1c** were calculated at the mPW1PW91/6-311++G(2d,2p) level with the PCM model in methanol based on the B3LYP/6-311+G(d)-optimized geometries (Supporting Information, Tables S1 and S2).[12,15] The calculated specific rotation (+53.32) of **1a** was close to the experimental value ($[\alpha]^{25}_D$ +24.7, *c* 0.08, MeOH), while the calculation data for **1c**(−27.18) had the opposite sign to the experimental value. Although the optical rotation is more variable, the sign of ORD does not change, and this rule was applied to solve this problem. Furthermore, +53.32 is considered similar to +24.7 in this context, but −27.18 is quite different, thereby permitting the absolute configuration of compound **1** to be identified. The absolute configuration of **1** was suggested to be 2*S*,5*S*,6*S*,9*S*,17*R*.

Tricholopardin B (**2**) was obtained as a colorless oil. Its HRESIMS data indicated its molecular formula is $C_{17}H_{26}O_4$. The IR absorption bands at 3443, 3429, and 1738 cm^{-1} revealed the presence of OH and C=O functionalities. A total of 17 carbon resonances were detected from the ^{13}C NMR and DEPT data (Table 1). The signals for a carbonyl carbon and four olefinic carbons, along with analysis of the MS data, indicated **2** has a bicyclic core. The $^1H-^1H$ COSY data indicated the three spin systems shown in bold lines in Figure 3. Preliminary analyses of the HMBC cross-peaks suggested that **2** possessed a cyclohexane with an exocyclic double bond and a γ-lactone in conjugation with a double bond. Detailed analysis of the 1D and 2D NMR data indicated that **2** might be a seco derivative of saponaceolide A.[1]

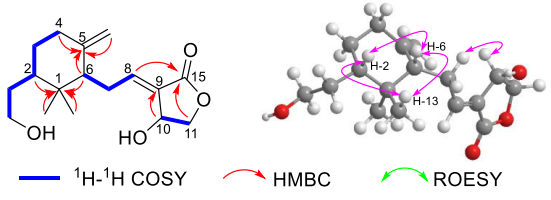

Figure 3. Key 2D NMR correlations of compound **2**.

The relative configuration of **2** was elucidated by an ROESY experiment (Figure 3). The ROESY cross-peaks of H-2/H-6, H-2/H_3-13, and H-6/H_3-13 suggested H-2, H-6, and Me-13 were cofacial, while the cross-peak of H-7/H-10 indicated that the double bond between C-8 and C-9 is in the *E*-configuration. However, the configuration of C-10 could not be determined from the ROESY data. Therefore, the theoretical ECD curve of **2** was calculated using the same method as was used for that of **1** (Figure 4). The calculated ECD spectra of **2** suggested the absolute configuration of C-10 in **2** to be *R*. However, the calculated ECD data suggested that the stereochemistry of C-2 and C-6 contributed little to the Cotton effects, and the absolute configurations of C-2 and C-6 could not be determined by the calculated ECD result. A proposed biosynthesis pathway for **2** suggested that the absolute configurations of C-2 and C-6 might be 2*S*,6*S*.

Compound **1** is a sesterterpene, and its biosynthetic pathway is supposed to start from the connection of a farnesyl pyrophosphate (FPP) unit with a geranyl pyrophosphate (GPP) unit. As shown in Scheme 1, the electrophilic attack of a formal carbocation at C-11 on the terminal double bond between C-1 and C-2 forms the C-2−C-11 linkage, rather than the C-1−C-11 linkage formed by a tail-to-tail coupling typically seen in the squalene biosynthesis derivatives, the common precursors of triterpenes. The C-2−C-11 linkage gives rise to a cyclohexane moiety and a fragment containing a pyran sharing a spiroketal carbon with the bridged heterocyclic system. Compound **2** might be derived from saponaceolide A by carbon−carbon bond cleavage. As far as we know, this type of terpenoid is only found in mushrooms of the genus *Tricholoma*, and there must be unique enzymes in the fruiting bodies of *Tricholoma* mushroom to produce the *Tricholoma* terpenoids.

In our recent studies, many terpenoids from mushrooms were found to inhibit NO production.[16−20] Therefore, compounds **1** and **2** were evaluated for their inhibitions on NO production in LPS-induced RAW264.7 macrophages. As a result, compound **1** exhibited potent inhibition with an IC_{50} of 0.08 μM, while compound **2** exhibited moderate activity with an IC_{50} value of 16.2 μM (positive control: MG-132, IC_{50} = 0.16 μM).

DOI: 10.1021/acs.jnatprod.8b00460
J. Nat. Prod. 2019, 82, 45−50

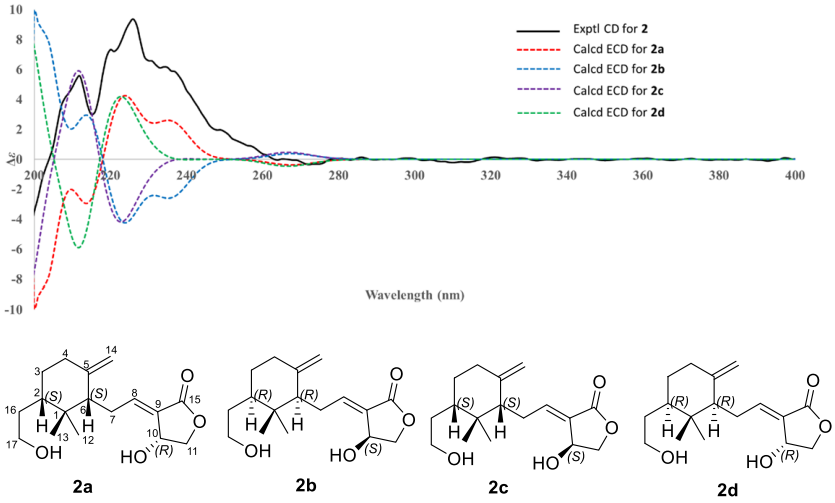

Figure 4. Comparison of the calculated ECD spectra for **2a**, **2b**, **2c**, and **2d** with the experimental spectrum of **2** in methanol with the PCM model.

Scheme 1. Proposed Biosynthetic Pathway for 1

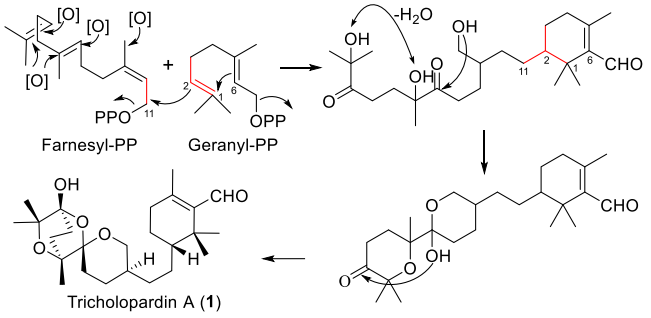

NO is an important cellular signaling molecule involved in many physiological and pathological processes.[21] It is also an important biological regulator and is therefore of fundamental interest in the fields of neuroscience, physiology, and immunology.[22] NO activates NF-κB in peripheral blood mononuclear cells, an important transcription factor in iNOS gene expression in response to inflammation.[23] Therefore, the potent inhibition of NO production by **1** was a direct indicator of its anti-inflammatory properties.

To thoroughly investigate its effect on NO production, further tests on the anti-inflammatory activities of **1** were performed. The effects of **1** on pro-inflammatory mediators, including TNF-α, IL-1β, and PGE2, were investigated in LPS-stimulated RAW264.7 and THP-1 cells. As depicted in Figure 5, the incubation of macrophages/monocytes with LPS alone for 24 h significantly increased the secretion of pro-inflammatory mediators TNF-α, IL-1β, and PGE2. However, pretreatment of the macrophages/monocytes with compound **1** at concentrations ranging of 2.5−20 μM suppressed ($p < 0.05$) the secretion of pro-inflammatory mediators compared to the LPS-only treatment in a dose-dependent manner. The inhibitory activities of compound **1** on the secretion of TNF-α, IL-1β, and PGE2 were 70.9%, 94.3%, and 92.5%, respectively, at 20 μM in LPS-induced RAW264.7 macrophages. Compound **1** suppressed the secretions of TNF-α and IL-1β by 99.9% and 99.3%, respectively, at 20 μM in LPS-induced THP-1 monocytes. In addition, compound **1** displayed low cytotoxicity to RAW 264.7 cells at concentrations up to 20 μM (with a cell viability of 60%), comparable to those of controls.

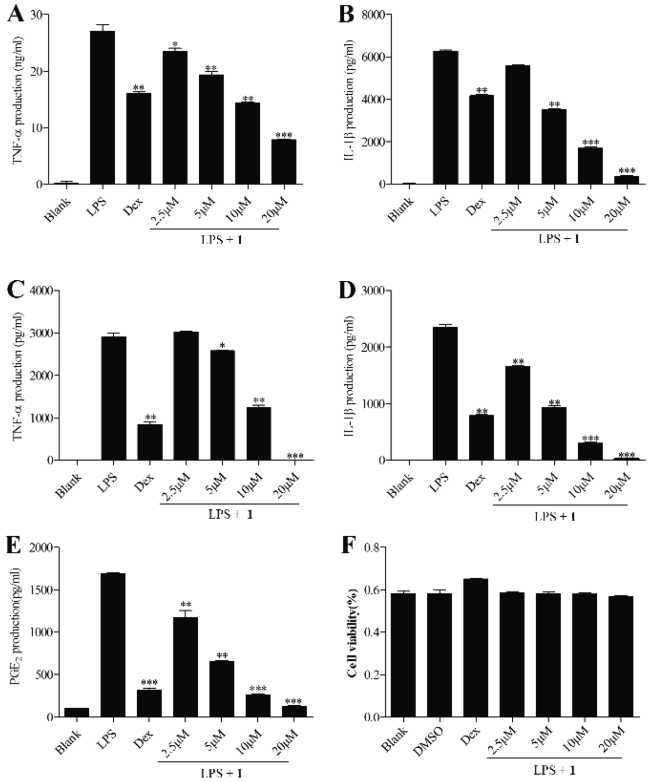

Figure 5. Effects of compound **1** on LPS-induced secretion of TNF-α (A) and IL-1β (B) in RAW 264.7 cell lines. Effects of compound **1** on TNF-α (C) and IL-1β (D) levels in LPS-stimulated THP-1 monocytes. Effects of compound **1** on PGE2 (E) and cell viability (F) in activated RAW 264.7 macrophages. Dexamethasone (Dex, 5 μM) was used as the positive control. Data are mean ± SD ($n = 3$) (*$P < 0.05$, **$P < 0.01$, and ***$P < 0.001$ vs LPS group).

EXPERIMENTAL SECTION

General Experimental Procedures. Melting points were obtained on an X-4 micro melting point apparatus. Optical rotations were measured with a Horiba SEPA-300 polarimeter. IR spectra were obtained with a Tenor 27 spectrophotometer using KBr pellets. 1D and 2D spectra were run on a Bruker Avance III 600 MHz spectrometer with tetramethylsilane as an internal standard. Chemical shifts (δ) were expressed in ppm with reference to the solvent signals.

DOI: 10.1021/acs.jnatprod.8b00460
J. Nat. Prod. 2019, 82, 45−50

Mass spectra were recorded on an Agilent 6200 Q-TOF MS system. Column chromatography (CC) was performed on silica gel (200−300 mesh, Qingdao Marine Chemical Ltd., Qingdao, People's Republic of China), RP-18 gel (20−45 μm, Fuji Silysia Chemical Ltd., Japan), and Sephadex LH-20 (Pharmacia Fine Chemical Co., Ltd., Sweden). Medium-pressure liquid chromatography (MPLC) was performed on a Büchi Sepacore System equipped with a C-615 pump manager, C-605 pump modules, and C-660 fraction collector (Büchi Labortechnik AG, Flawil, Switzerland) and columns packed with RP-18 gel. Preparative high-performance liquid chromatography (prep-HPLC) was performed on an Agilent 1260 liquid chromatography system equipped with Zorbax SB-C_{18} columns (5 μm, 9.4 mm × 150 mm or 21.2 mm × 150 mm) and a DAD detector. Fractions were monitored by TLC (GF 254, Qingdao Haiyang Chemical Co., Ltd. Qingdao), and spots were visualized by heating silica gel plates sprayed with 10% H_2SO_4 in EtOH.

Fungal Material. Wild mushrooms, *Tricholoma pardinum*, were collected from Schwarzwald in southwestern Germany in October 2014 and identified by Prof. Yu-Cheng Dai of Beijing Forestry University. A voucher specimen (No. HPCF20141008.6) was deposited at the School of Pharmaceutical Sciences, South-Central University for Nationalities.

Extraction and Isolation. The air-dried fruiting bodies of *T. pardinum* (1.5 kg) were extracted with MeOH (24 h × 3) and then partitioned with H_2O and EtOAc (1:1). Finally, an EtOAc extract (56 g) was obtained, which was submitted to silica gel CC using $CHCl_3$−MeOH (from 1:0 to 0:1) to give eight fractions (A−H). Fraction D (2.3 g) was separated by silica gel CC using petroleum ether−acetone (10:1−4:1, v/v) to afford five subfractions (D1−D5). Fraction D3 (18 mg) was purified by HPLC (MeCN−H_2O from 80:20 to 95:5, v/v, 25 min) to afford compound **1** (3.2 mg). Fraction D5 (117 mg) was purified by HPLC (MeCN−H_2O from 70:30 to 90:10, v/v, 20 min) to afford compound **2** (6.8 mg).

*Tricholopardin A (**1**):* colorless oil; $[\alpha]^{25}_D$ +24.7 (*c* 0.08, MeOH); UV (MeOH) λ_{max} (log ε) 224 (3.26), 206 (4.54) nm; IR (KBr) ν_{max} 3440, 2946, 1717, 1640, 1376, 1245, 1077, 994 cm^{-1}; ^1H and ^{13}C NMR data, see Table 1; positive ion HRESIMS *m*/*z* 459.2512 $[M + K]^+$ (calcd for $C_{25}H_{40}O_5K$ 459.2507).

*Tricholopardin B (**2**):* colorless oil; $[\alpha]^{25}_D$ +34.7 (*c* 0.34, MeOH); UV (MeOH) λ_{max} (log ε) 222 (3.35), 206 (3.88) nm; IR (KBr) ν_{max} 3443, 3429, 2947, 1738, 1631, 1368, 1087, 1022, 998 cm^{-1}; ^1H and ^{13}C NMR data, see Table 1; positive ion HRESIMS *m*/*z* 317.1714 $[M + Na]^+$ (calcd for $C_{17}H_{26}O_4Na$ 317.1723).

Nitric Oxide Production in RAW 264.7 Macrophages. Murine monocytic RAW264.7 macrophages were dispensed into 96-well plates (2 × 10^5 cells/well) containing RPMI 1640 medium (HyClone) with 10% fetal bovine serum (FBS) under a humidified atmosphere with 5% CO_2 at 37 °C. After 24 h of preincubation, cells were treated with serial dilutions of the test compound, up to a maximum concentration of 25 μM, in the presence of 1 μg/mL LPS for 18 h. The compound was dissolved in DMSO and further diluted in medium to produce different concentrations. NO production in each well was assessed by adding 100 μL of Griess reagent (reagent A and reagent B, Sigma) to 100 μL of each supernatant from the LPS (Sigma)-treated or LPS- and compound-treated cells in triplicate. After a 5 min incubation, the absorbance of samples was measured at 570 nm with a 2104 Envision multilabel plate reader (PerkinElmer Life Sciences, Inc., Boston, MA, USA). MG-132 (Sigma) was used as a positive control (IC_{50} = 0.16 μM).

Effect of Compound 1 on Pro-inflammatory Mediators. Three inflammatory mediators, namely, TNF-α, IL-1β, and PGE2, were used to investigate the anti-inflammatory effect of **1** in LPS-stimulated RAW264.7 and THP-1 cells. RAW 264.7 and THP-1 cells were obtained from the Kunming cell bank of the Chinese Academy of Sciences (Kunming, China). Cells were cultured at 37 °C and respectively maintained in DMEM and RPMI 1640 media containing 10% heat inactivated FBS and 1% penicillin in a humidified 5% CO_2 atmosphere. RAW 264.7 macrophages were detached by trypsin-EDTA and seeded in a 96-well plate for the viability assay. Compound **1** was dissolved in dimethyl sulfoxide (DMSO) and was used for the treatment of cells. Cells grown to 80% confluence were pretreated with compound **1** (2.5−20 μM). Cell viability of compound **1** was measured by CellTiter 96 Queous One Solution cell proliferation assay reagent following the manufacturer's instruction (MTS).

Determination of Cytokine Levels in LPS-Induced RAW 264.7 and THP-1 Cells. RAW 264.7 and THP-1 cells were pretreated with compound **1** (2.5−20 μM) or dexamethasone (5 μM) for 30 min before LPS (1 μg/mL) stimulation for 24 h. Dexamethasone is a synthetic glucocorticoid that suppresses cytokine responses and was used as a positive control. Supernatants were collected, and the production of TNF-α, IL-1β, and PGE2 was assayed using enzyme linked immunosorbent assay (ELISA) kits (BD Biosciences, USA) according to the manufacturer's instructions.

Data were expressed as means ± SD (*n* = 3). Differences between means of each group were assessed by one-way analysis of variance followed by Dunnett's T3 test and a two-tailed Student's *t* test. All analyses were conducted using GraphPad Prism 5.0 software. A *P*-value < 0.05 was considered statistically significant.

ECD Calculation. Conformation searches based on molecular mechanics with MMFF94S force fields were performed for (2*S*,5*S*,6*S*,9*S*,17*R*)-**1** (**1a**), (2*S*,5*S*,6*S*,9*S*,17*S*)-**1** (**1b**), (2*R*,5*R*,6*R*,9*R*,17*R*)-**1** (**1c**), and (2*R*,5*R*,6*R*,9*R*,17*S*)-**1** (**1d**) and gave 21, 25, 25, and 21 stable conformers with distributions higher than 1%, respectively.[24,25] All these conformers were further optimized by the density functional theory method at the B3LYP/6-311G+(d) level by the Gaussian 09 program package.[26] The ECDs were calculated using the CAM-B3LYP/6-311G+(d,p) level in methanol with the PCM model on CAM-B3LYP/6-311G+(d,p). The calculated ECD curves and weighted ECD were all generated using SpecDis 1.60 with σ = 0.3 eV and a UV shift of 10 nm, respectively.[27]

Specific Rotation Calculation. The specific rotation calculations for compounds (2*S*,5*S*,6*S*,9*S*,17*R*)-**1** (**1a**) and (2*R*,5*R*,6*R*,9*R*,17*R*)-**1** (**1c**) were performed using Gaussian 09 (Supporting Information). The conformers **1aA**−**1aU** and **1cA**−**1cY** were optimized at the B3LYP/6-311+G(d) level, all of which were subjected to specific rotation calculations at the mPW1PW91/6-311++G(2d,2p) level in methanol with the PCM model. The calculated specific rotation data of these conformers were averaged according to the Boltzmann distribution theory.

■ ASSOCIATED CONTENT

Supporting Information

The Supporting Information is available free of charge on the ACS Publications website at DOI: 10.1021/acs.jnatprod.8b00460.

Spectroscopic data including 1D and 2D NMR and HRMS (PDF)

Computational details of **1** and **2** (PDF)

■ AUTHOR INFORMATION

Corresponding Authors

*E-mail: 2015051@mail.scuec.edu.cn (Z.-H. Li).

*E-mail: jkliu@mail.kib.ac.cn (J.-K. Liu).

ORCID

Tao Feng: 0000-0002-1977-9857

He-Ping Chen: 0000-0003-0416-9535

Yong-Sheng Zheng: 0000-0002-1019-5521

Zheng-Hui Li: 0000-0003-1284-0288

Ji-Kai Liu: 0000-0001-6279-7893

Notes

The authors declare no competing financial interest.

■ ACKNOWLEDGMENTS

This work was financially supported by the National Natural Science Foundation of China (81872762, 31870513,

DOI: 10.1021/acs.jnatprod.8b00460
J. Nat. Prod. 2019, 82, 45−50

81561148013, 21502239), the Key Projects of Technological Innovation of Hubei Province (2016ACA138), and the Fundamental Research Funds for the Central University, South-Central University for Nationalities (CZP18005, CZT18013, CZT18014). The authors thank Analytical & Measuring Centre, South-Central University for Nationalities, for the spectra measurements. The computational work was partially supported by the HPC of Kunming Institute of Botany and the Supercomputing Environment of Chinese Academy of Science (ScGrid).

REFERENCES

(1) De Bernardi, M.; Garlaschelli, L.; Gatti, G.; Vidari, G.; Finzi, P. V. *Tetrahedron* **1988**, *44*, 235−240.
(2) De Bernardi, M.; Garlaschelli, L.; Toma, L.; Vidari, G.; Vita-Finzi, P. *Tetrahedron* **1991**, *47*, 7109−7116.
(3) De Bernardi, M.; Garlaschelli, L.; Toma, L.; Vidari, G.; Vita-Finzi, P. *Tetrahedron* **1992**, *48*, 187.
(4) Yoshikawa, K.; Kuroboshi, M.; Arihara, S.; Miura, N.; Tujimura, N.; Sakamoto, K. *Chem. Pharm. Bull.* **2002**, *50*, 1603−1606.
(5) Vidari, G.; Franzini, M.; Garlaschelli, L.; Maronati, A. *Tetrahedron Lett.* **1993**, *34*, 2685−2688.
(6) Trost, B. M.; Corte, J. R. *Angew. Chem., Int. Ed.* **1999**, *38*, 3664−3666.
(7) Trost, B. M.; Corte, J. R.; Gudiksen, M. S. *Angew. Chem., Int. Ed.* **1999**, *38*, 3662−3664.
(8) Vidari, G.; Lanfranchi, G.; Pazzi, N.; Serra, S. *Tetrahedron Lett.* **1999**, *40*, 3063−3066.
(9) Vidari, G.; Pazzi, N.; Lanfranchi, G.; Serra, S. *Tetrahedron Lett.* **1999**, *40*, 3067−3070.
(10) Yin, X.; Feng, T.; Shang, J. H.; Zhao, Y. L.; Wang, F.; Li, Z. H.; Dong, Z. J.; Luo, X. D.; Liu, J. K. *Chem. - Eur. J.* **2014**, *20*, 7001−7009.
(11) Feng, T.; He, J.; Ai, H.-L.; Huang, R.; Li, Z. H.; Liu, J. K. *Nat. Prod. Bioprospect.* **2015**, *5*, 205−208.
(12) Zhao, Z. Z.; Chen, H. P.; Wu, B.; Zhang, L.; Li, Z. H.; Feng, T.; Liu, J. K. *J. Org. Chem.* **2017**, *82*, 7974−7979.
(13) Guillen, P. O.; Jaramillo, K. B.; Genta-Jouve, G.; Sinniger, F.; Rodriguez, J.; Thomas, O. P. *Org. Lett.* **2017**, *19*, 1558−1561.
(14) Zhang, D. W.; Zhao, L. L.; Wang, L. N.; Fang, X. M.; Zhao, J. Y.; Wang, X. W.; Li, L.; Liu, H. Y.; Wei, Y. Z.; You, X. F.; Cen, S.; Yu, L. Y. *J. Nat. Prod.* **2017**, *80*, 371−376.
(15) Stephens, P. J.; Devlin, F. J.; Cheeseman, J. R.; Frisch, M. J. *J. Phys. Chem. A* **2001**, *105*, 5356−5371.
(16) Zhang, S. B.; Li, Z. H.; Stadler, M.; Chen, H. P.; Huang, Y.; Gan, X. Q.; Feng, T.; Liu, J. K. *Phytochemistry* **2018**, *152*, 105−112.
(17) Chen, H. P.; Zhao, Z. Z.; Li, Z. H.; Huang, Y.; Zhang, S. B.; Tang, Y.; Yao, J. N.; Chen, L.; Isaka, M.; Feng, T.; Liu, J. K. *J. Agric. Food Chem.* **2018**, *66*, 3146−3154.
(18) Feng, T.; Li, X. M.; He, J.; Ai, H. L.; Chen, H. P.; Li, X. N.; Li, Z. H.; Liu, J. K. *Org. Lett.* **2017**, *19*, 5201−5203.
(19) Feng, T.; Cai, J. L.; Li, X. M.; Zhou, Z. Y.; Li, Z. H.; Liu, J. K. *J. Agric. Food Chem.* **2016**, *64*, 1945−1949.
(20) Feng, T.; Cai, J. L.; Li, X. M.; Zhou, Z. Y.; Huang, R.; Zheng, Y. S.; Li, Z. H.; Liu, J. K. *Tetrahedron Lett.* **2016**, *57*, 3544−3546.
(21) Hou, Y. C.; Janczuk, A.; Wang, P. G. *Curr. Pharm. Design* **1999**, *5*, 417−441.
(22) Culotta, E.; Koshland, D. E., Jr *Science* **1992**, *258*, 1862−1864.
(23) Kaibori, M.; Sakitani, K.; Oda, M.; Kamiyama, Y.; Masu, Y.; Okumura, T. *J. Hepatol.* **1999**, *30*, 1138−1145.
(24) Chianese, G.; Silber, J.; Luciano, P.; Merten, C.; Erpenbeck, D.; Topaloglu, B.; Tasdemir, D. *J. Nat. Prod.* **2017**, *80*, 2566−2571.
(25) Goto, H.; Osawa, E. *J. Am. Chem. Soc.* **1989**, *111*, 8950−8951.
(26) Goto, H.; Osawa, E. *J. Chem. Soc., Perkin Trans. 2* **1993**, *2*, 187−198.
(27) Frisch, M. J. T. G. W.; Schlegel, H. B.; Scuseria, G. E.; Robb, M. A.; Cheeseman, J. R.; Scalmani, G.; Barone, V.; Mennucci, B.; Petersson, G. A.; Nakatsuji, H.; Caricato, M.; Li, X.; Hratchian, H. P.; Izmaylov, A. F.; Bloino, J.; Zheng, G.; Sonnenberg, J. L.; Hada, M.; Ehara, M.; Toyota, K.; Fukuda, R.; Hasegawa, J.; Ishida, M.; Nakajima, T.; Honda, Y.; Kitao, O.; Nakai, H.; Vreven, T.; Montgomery, J. A., Jr.; Peralta, J. E.; Ogliaro, F.; Bearpark, M.; Heyd, J. J.; Brothers, E.; Kudin, K. N.; Staroverov, V. N.; Keith, T.; Kobayashi, R.; Normand, J.; Raghavachari, K.; Rendell, A.; Burant, J. C.; Iyengar, S. S.; Tomasi, J.; Cossi, M.; Rega, N.; Millam, J. M.; Klene, M.; Knox, J. E.; Cross, J. B.; Bakken, V.; Adamo, C.; Jaramillo, J.; Gomperts, R.; Stratmann, R. E.; Yazyev, O.; Austin, A. J.; Cammi, R.; Pomelli, C.; Ochterski, J. W.; Martin, R. L.; Morokuma, K.; Zakrzewski, V. G.; Voth, G. A.; Salvador, P.; Dannenberg, J. J.; Dapprich, S.; Daniels, A. D.; Farkas, O.; Foresman, J. B.; Ortiz, J. V.; Cioslowski, J.; Fox, D. J. *Gaussian 09*, revision D. 01; Gaussian, Inc.: Wallingford, CT, 2010.

DOI: 10.1021/acs.jnatprod.8b00460
J. Nat. Prod. 2019, 82, 45−50